Journal of Marine Systems 78 (2009) S306–S320

Contents lists available at ScienceDirect

Journal of Marine Systems

journal homepage: www.elsevier.com/locate/jmarsys

At-sea real-time coupled four-dimensional oceanographic and acoustic forecasts during Battlespace Preparation 2007

Frans-Peter A. Lam [a,*], Patrick J. Haley Jr. [b], Jeroen Janmaat [a], Pierre F.J. Lermusiaux [b,*], Wayne G. Leslie [b], Mathijs W. Schouten [a], Lianke A. te Raa [a], Michel Rixen [c]

[a] Netherlands Organisation for Scientific Applied Research (TNO), business unit Observation Systems, The Hague, The Netherlands
[b] Massachusetts Institute of Technology (MIT), Department of Mechanical Engineering, Cambridge, USA
[c] NATO Undersea Research Centre (NURC), La Spezia, Italy

ARTICLE INFO

Article history:
Received 27 June 2008
Received in revised form 15 September 2008
Accepted 22 January 2009
Available online 1 March 2009

ABSTRACT

Systems capable of forecasting ocean properties and acoustic performance in the littoral ocean are becoming a useful capability for scientific and operational exercises. The coupling of a data-assimilative nested ocean modeling system with an acoustic propagation modeling system was carried out at sea for the first time, within the scope of Battlespace Preparation 2007 (BP07) that was part of Marine Rapid Environmental Assessment (MREA07) exercises. The littoral region for our studies was southeast of the island of Elba (Italy) in the Tyrrhenian basin east of Corsica and Sardinia. During BP07, several vessels collected in situ ocean data, based in part on recommendations from oceanographic forecasts. The data were assimilated into a four-dimensional high-resolution ocean modeling system. Sound-speed forecasts were then used as inputs for bearing- and range-dependent acoustic propagation forecasts. Data analyses are carried out and the set-up of the coupled oceanographic–acoustic system as well as the results of its real-time use are described. A significant finding is that oceanographic variability can considerably influence acoustic propagation properties, including the probability of detection, even in this apparently quiet region around Elba. This strengthens the importance of coupling at-sea acoustic modeling to real-time ocean forecasting. Other findings include the challenges involved in downscaling basin-scale modeling systems to high-resolution littoral models, especially in the Mediterranean Sea. Due to natural changes, global human activities and present model resolutions, the assimilation of synoptic regional ocean data is recommended in the region.

1. Introduction

Much progress has been made in recent years towards the coupling of data-assimilative, four-dimensional oceanographic modeling with two-dimensional acoustic propagation modeling. A first major integrated ocean–acoustic field study occurred in Middle Atlantic Bight shelfbreak region (Lynch et al., 1997). In addition to integrated data collection, this study involved acoustic and realistic oceanographic modeling, but the two modeling activities were not coupled. Concepts of realistic data-assimilative ocean modeling directly coupled with acoustic propagation modeling were developed through the Capturing Uncertainty research initiative, including the efforts of the "UNcertainties and Interdisciplinary Transfers through the End-to-End System" team (Abbot and Dyer, 2002; Lermusiaux et al., 2002a; Robinson et al., 2002). A review of coupled oceanographic–acoustic and end-to-end system research is provided by Robinson and Lermusiaux (2004). The first time coupled acoustic–ocean forecasts and advanced data assimilation were carried out in real-time was in 2005 (Wang et al., 2009-this volume). This was followed by other related onshore efforts in subsequent years (Haley et al., 2009; Xu et al., 2008). A new application result reported in this manuscript is that such realistic coupling has now been done at sea. Specifically, 2D-acoustic and data-assimilative 3-D-ocean forecasts were coupled and carried out in real-time for the first time aboard a naval vessel, with onshore support for expert guidance and specific on-demand simulations.

Our effort was carried out as part of the Battlespace Preparation exercises in collaboration with the NATO Undersea Research Center (NURC). One of the objectives of these exercises was to expand on Marine Rapid Environmental Assessment (MREA) research (Pouliquen et al., 1997; Kirwan and Robinson, 1997; Robinson and Sellschopp, 2002) by combining remote sensing, in situ and autonomous sensors with coupled numerical models to produce a

* Corresponding authors.
E-mail addresses: frans-peter.lam@tno.nl (F.-P.A. Lam), pierrel@mit.edu (P.F.J. Lermusiaux).

0924-7963/$ – see front matter © 2009 Elsevier B.V. All rights reserved.
doi:10.1016/j.jmarsys.2009.01.029

real-time environmental representation. The MREA 2007 program included the BP07 exercise, which took place mostly south of Elba, and the Ligurian Air-Sea Interaction Experiment to the north.

The Battlespace Preparation 2007 (BP07) sea exercise occurred in April/May 2007. It was a multi-ship, multi-institutional, multi-disciplinary cooperative experiment focused on the establishment of an integrated 4-D Recognized Environmental Picture of a shallow-water environment in support of two types of naval operations: anti-submarine warfare and amphibious operations. Both types of operations strongly benefit from an accurate and timely assessment of the geophysical state of the operational location and its immediate surroundings. This work is part of the general BP07 effort on ocean–acoustic coupling, characterization and prediction. Rixen et al. (2009–this issue) investigate the use of dynamic super-ensemble prediction techniques based on the Kalman filter (Kalman, 1960) to allow for a temporal evolution of model combinations and provide a thorough acoustic propagation sensitivity study to assess the potential of super-ensemble predictions for acoustic inversion and tomography purposes. Carriere et al. (2009–this issue) investigate full-field tomography and Kalman tracking of the range-dependent sound speed for the same field experiment.

The operational area for BP07 was southeast of Elba (Italy) in the Tyrrhenian basin east of Corsica and Sardinia (see Fig. 1 to be discussed in Section II). Elba lies off the western coast of Italy in the Corsica Channel, which connects the Ligurian Sea to the north with the Tyrrhenian Sea to the south. This area has been a test-bed for the development of the NATO Tactical Ocean Modeling System (Coelho and Robinson, 2003; Coelho et al., 2004; Rixen and Ferreira-Coelho, 2006, 2007; Rixen et al., 2008) having been utilized for a number of previous MREA exercises. The MREA concept and its application are well documented (Coelho and Rixen, 2008; Allard et al., 2008; Ko et al., 2008; Rixen et al., 2008).

In this paper, we describe the results of the on-board operational oceanographic and acoustic modeling component of the exercise. In Section 2, an introduction to the general environment in which the BP07 exercise was embedded is given, along with a summary of our prior experience in this region. The data collection strategy, the results of the data analysis and the components of the new coupled data-driven oceanographic and acoustic modeling system are given in Section 3. Selected results of the real-time activities in the field during the exercise, including some of our coupled ocean–acoustic products issued at sea for the first time, are discussed in Section 4. The importance of mixed layer dynamics for acoustic predictions in the summer is stressed as well as the challenges involved in utilizing high-resolution data-assimilative models to downscale basin-scale ocean modeling estimates to small coastal regions. The conclusions and recommendations are in Section 5.

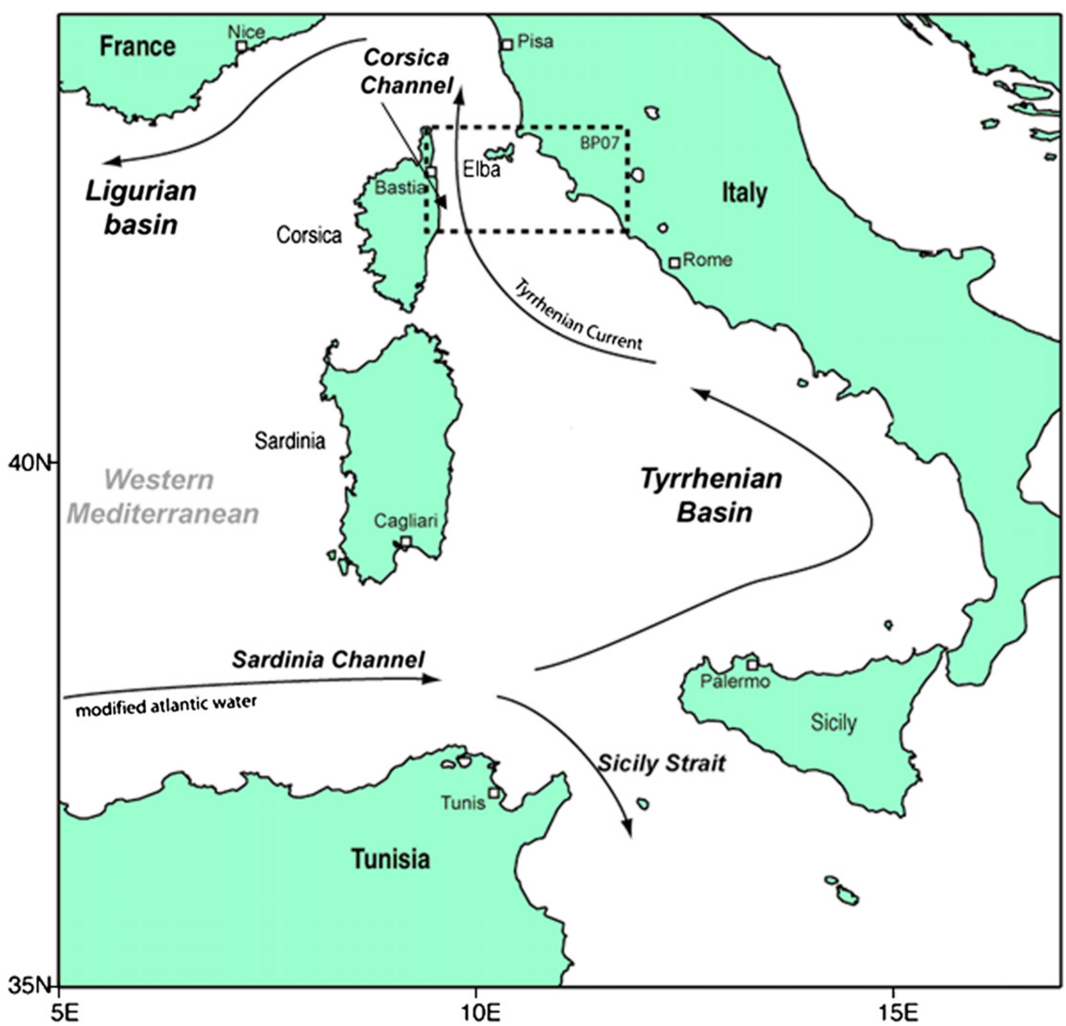

Fig. 1. Geographical setting of the experiment in the Western Mediterranean Sea. A crude schematic of the mean surface circulation of the Modified Atlantic Water is added to place the regional flow in its larger context (circulation after (Millot, 1999)). It should be noted that the flow in the Mediterranean is highly variable and unstable. The dashed rectangular box denotes the region modeled during the BP07 experiment.

2. General oceanographic environment and prior regional experience

The dominant large scale general circulation feature in the operational area (Fig. 1) is the Tyrrhenian Current, which flows northward along the eastern coast of Corsica, through the Corsica Channel into the Ligurian Sea (Astraldi and Gasparini, 1992, 1994). Coastal currents are generally directed from east to west, but sometimes reverse for short periods corresponding to the passage of intense lows. Seasonal variability is observed, with more intense currents during winter (Artale et al., 1994). Mesoscale variability is forced by local wind events. Cool regions along the coast result from upwelling. For similar operational scenarios, tidal effects (e.g. Lam et al., 2004; Gerkema et al., 2004) are often of significant importance for acoustic applications. This is especially the case when tides are causing a transition towards small scale processes into the deeper ocean (Maas et al., 1997). However, tides are not significant in this area, while inertial oscillations often occur.

The Tyrrhenian Sea exchanges water with the rest of the Mediterranean Sea through the Sardinia Channel, the Sicily Strait and the Corsica Channel. The surface water (0–200 m) entering the Tyrrhenian Sea through the Sardinia Channel is Modified Atlantic Water (MAW). The MAW is characterized by relatively low salinity (generally less than 38 PSU), and flows cyclonically along the Italian coast. MAW can reach the Ligurian Sea through the Corsica channel. There is inflow of Levantine Intermediate Water (LIW), which is marked by a subsurface temperature maximum and by a higher salinity (on average 38.8 PSU), through the Sicily Strait, deeper than 200 m down to about 700 m (Astraldi et al., 2002; André et al., 2005; Gasparini et al., 2005). As the BP07 area is generally shallower than 500 m, no deep Mediterranean water would be expected. Data from a previous NURC exercise (ASCOT-02; May 2002) indicated the presence of a 30–40 m deep mixed layer and a sound velocity minimum in the 40–70 m depth range.

Our prior modeling experience in this region includes successful participation in four exercises. The first one was GOATS-2000 (Onken et al., 2005), during which ocean nowcasts, forecasts and adaptive sampling guidance were provided and inter-model nested operations demonstrated. The second, ASCOT-02 (Coelho et al., 2004), was part of a series of Coastal Predictive Skill Experiments focused on quantitative forecast skill evaluation and forecast system development in the region. In the third, MREA03, an experiment was carried out to characterize sub-mesoscale/inertial dynamics in an area of the channel north of Elba. A new idea there was to initialize, forecast and update small, high-resolution (sub-mesoscale) domains focusing on areas of observations and/or tactical interest. This rapid forecast capability leads to the potential for real-time adaptive modeling (Lermusiaux, 2007), reducing local uncertainty and improving tactical forecasting (Leslie et al., 2008). Model errors can also be learned in real-time (Logutov and Robinson, 2005). During the fourth, FAF05 (Wang et al., 2006, 2009-this volume), we developed new algorithms and software for the coupling the real-time ocean environmental modeling, uncertainty prediction and adaptive sampling. For adaptive rapid environmental assessment, physical–acoustical adaptive sampling recommendations were issued every day, aiming to capture the vertical variability of the thermocline (due to fronts, eddies, internal waves, etc) and to minimize the corresponding uncertainties.

3. Data analysis and data-driven oceanographic–acoustic modeling system

3.1. Oceanographic data collection and data analysis

During the April 22 to May 5, 2007 BP07 sea exercise, numerous resources were utilized to provide an integrated environmental characterization. In addition to Italian Navy assets, the Royal Netherlands Navy (RNLN) was present with the HNLMS Snellius, its launch (a support vessel of 9.5 m length) and its rigid-hull inflatable boat (RHIB) for hydrographic sampling and acoustic surveillance. With the NURC coastal research vessel R/V Leonardo, 16 days of almost continuous oceanographic, hydrographic and acoustic measurements were collected in the area of interest and its dynamical region of influence (Fig. 2).

The planned data collection for the dynamical region of influence aimed to cover the full region with hydrographic observations just before the exercise. The plan included relatively sparsely located stations in the outer parts of the domain, and increasingly denser coverage zooming in on the coastal region (Fig. 2, left). Such data sets are needed for model initialization and for capturing the larger-scale ocean features in the region (strength of the coastal currents, main eddies, etc). Data collected during the exercise is then assimilated to reduce forecast uncertainties (Lermusiaux et al., 2006a). Forecast uncertainties are due to errors in atmospheric forcing forecasts, to the ocean model itself and to the own predictability limit of the ocean. Specifically, uncertainties depend on the level of detail provided in the initial conditions and on the resolution of the model used and the scales considered.

Because of mechanical problems with the Italian Navy vessel, a smaller alternative initialization data collection plan was designed in real-time (Fig. 2, right). These data were collected by two other major vessels participating in other activities during the exercise. Even though the initialization region was substantially decreased, and covered during the first week of the exercise, by April 29, good coverage of the new, smaller, initialization region was achieved (Fig. 2, right).

Primary data acquisition was done by sampling with a Conductivity–Temperature–Depth (CTD) sensor, yielding profiles of temperature and salinity, hence density and pressure. A total of 70 CTD casts were collected up to April 29. These data were sent from the ship to the NURC exercise web site. From the NURC site the data was downloaded, quality controlled and re-formatted for model initialization. Additional temperature information was collected by a Moving Vessel Profiler (MVP) available on the HNLMS Snellius. This

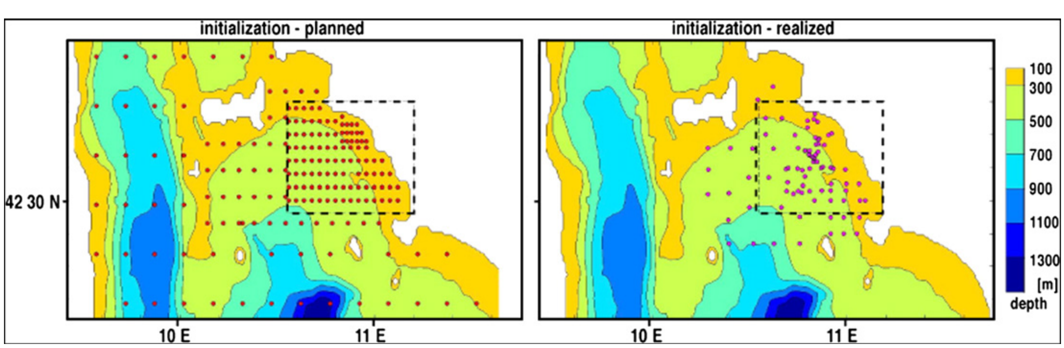

Fig. 2. CTD station positions: planned (left) and accomplished by April 29 (right).

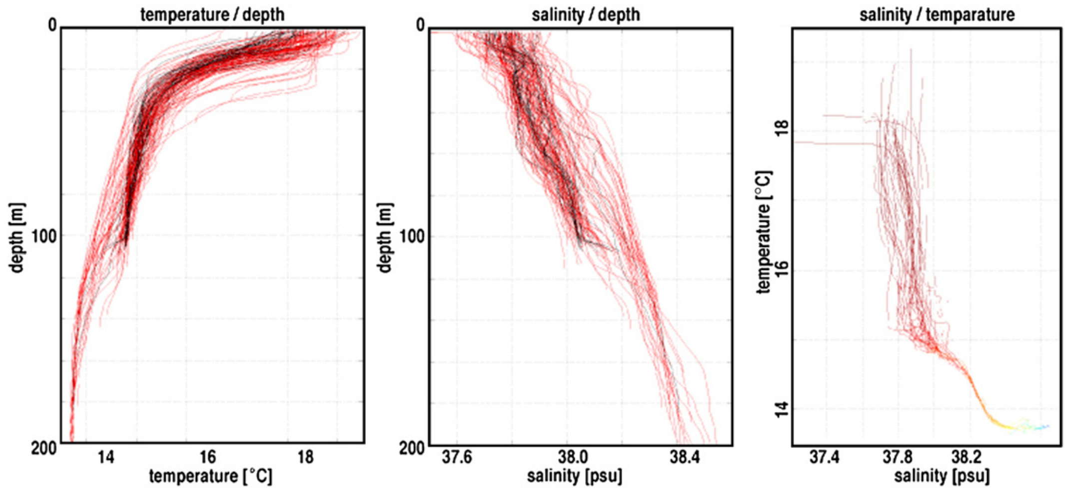

Fig. 3. CTD profiles collected during BP07. (Left) Temperature vs. depth. (Center) Salinity vs. depth. (Right) Temperature vs. salinity.

autonomously functioning profiler has sensors for pressure, temperature and sound velocity, and is normally used for calibrating the acoustic measurements for the sound velocity profile. We mainly used the temperature samples to increase the density of the grid of observed temperature profiles.

The CTD profiles are plotted in Fig. 3. The data generally indicate a mixed layer of 5–10 m, although a handful of stations, located in the southwest, have a mixed layer which extends to 30 m. On average, the mixed layer is much shallower than was observed in 2002. The 2002 exercise took place in late May to early June, while BP07 was in late April to early May. A shallow mixed layer has an important impact on the acoustic propagation since it changes the main depth of refraction and for very small mixed layer this often means that the whole water column is ensonified up to the wavy ocean surface, leading to surface refractions and other random surface effects. For certain source-target-receiver configurations, however, the mixed layer depth can be less sensitive. At 90 m, temperatures drop dramatically, suggesting the transition between Modified Atlantic Water and Levantine Intermediate Water (Warn-Varnas et al., 1999; Lermusiaux and Robinson, 2001; Onken et al., 2003). The T/S plot indicates that the primary variability in the water masses of the area is contained above 100 m.

From these data, an initial field was created by smooth interpolation with mesoscale horizontal decorrelation scales (25 km decay scale, with a zero crossing scale of 50 km) and temporal decorrelation scale (3 weeks). The assimilation fields were formed with much smaller scales, especially in time, to allow for the time dependence of the initialization run. Both spatial correlation functions have been plotted in Fig. 4.

The additional value of the MVP is assessed from Fig. 5. From the error figures (lower two panels), it is clear that outside the well-sampled region (between the islands in Fig. 2) little improvement is possible. Importantly, for the addition of the MVP data allows to reach a non-dimensional error estimate smaller than 0.2 for most of the simulation domain. The region colored red in the CTD-only panel should not be considered too realistic (error larger than 30%). We have found that since these locations are near the open-boundary, if the MVP data is not utilized, the initial fields near the open-boundaries are not accurate enough to lead to adequate simulations in the smaller intensive region of interest. It is only with this larger initial coverage that the open boundary condition scheme can provide good enough estimates as time advances in the simulation. Finally, MVP data are acquired very rapidly which is paramount for REA capabilities.

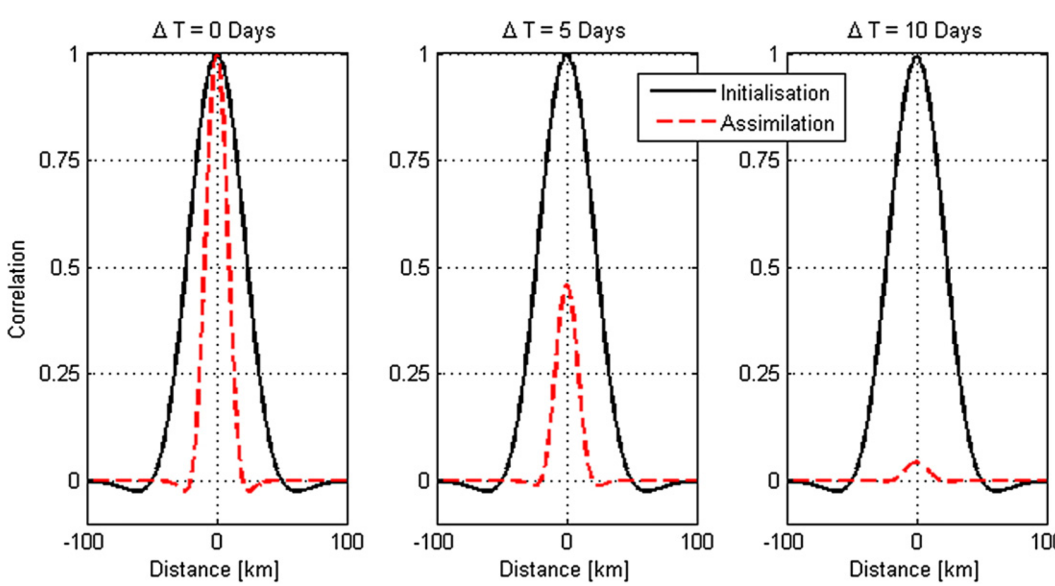

Fig. 4. Decorrelation scales for the initialization runs. All data are used twice: once heavily smoothed to start the initialization run, and once more sharply defined in both space and especially time, to constrain the variability in the initialization run.

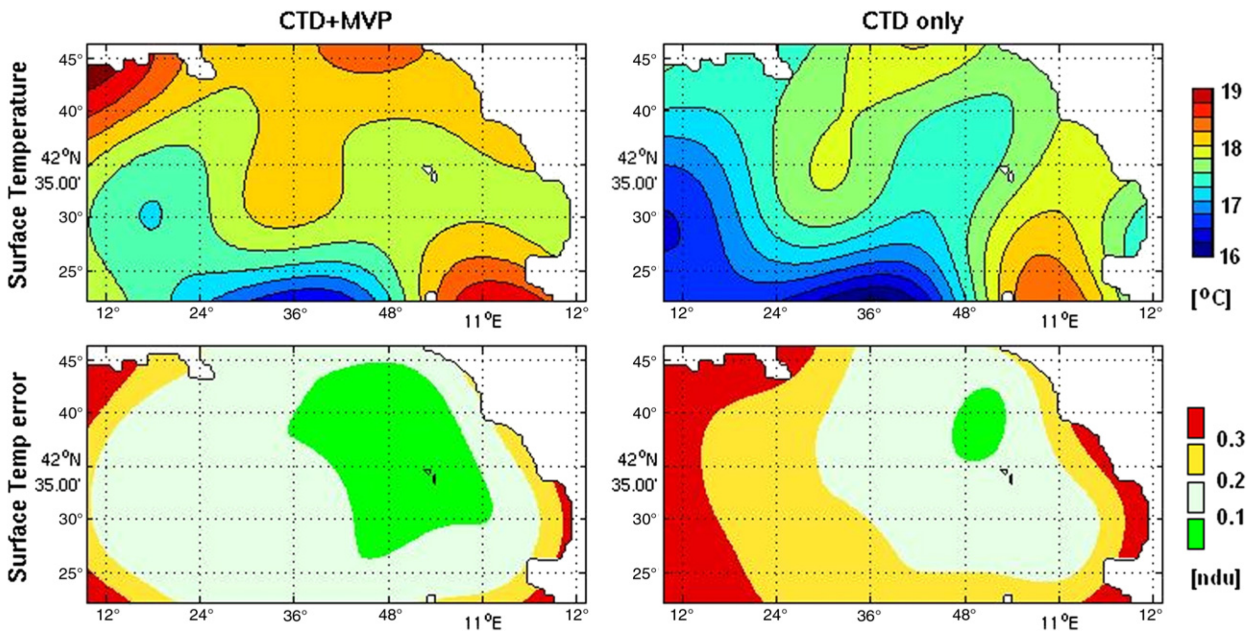

Fig. 5. Effect of MVP data on the optimal interpolation of surface temperature. Top: Temperatures (°C) from an OA with (left) and without (right) MVP data, based on the stations covered for the initialization (see upper two panels of Fig. 8 for station positions). Bottom: Associated error fields (dimensionless values): this is the posterior (residual) error of the OA map, assuming non-dimensional prior errors of 0.03 at data points and of 1.0 for the unknown field. The light gray-green region covers most of the domain due to the addition of the MVP data (bottom left panel), whereas the extrapolation of low temperatures towards the western and southwestern part of the domain is strongly reduced.

3.2. Data-driven oceanographic–acoustic modeling system

During BP07, we showcased a new real-time working process chain (Fig. 6) that we developed prior to the exercise. The system chain consists of the following interconnected components: in situ data collection, adaptively collected based on observed and predicted features; utilization of both the in situ and external data into nested ocean modeling domains to provide high-resolution oceanographic forecasts; and, use of these forecasts as inputs to the TNO sonar performance prediction tool, the Acoustic Loss Model for Operational Studies and Tasks (ALMOST, Schippers, 1995). The whole coupled system allowed us to provide high-resolution sonar performance nowcasts and predictions, up to several days ahead. All results were published on the internet and linked to by the central data server site at NURC to be available to all partners of the exercise.

It should be noted that the sonar performance is based on a single scenario and setup of transmitter and receiver array. For other scenarios, such as a change in the depth of the submarine to be detected, results may be different. The scenario was not tuned for its sensitivity to oceanographic variability. The submarine depth of 50 m

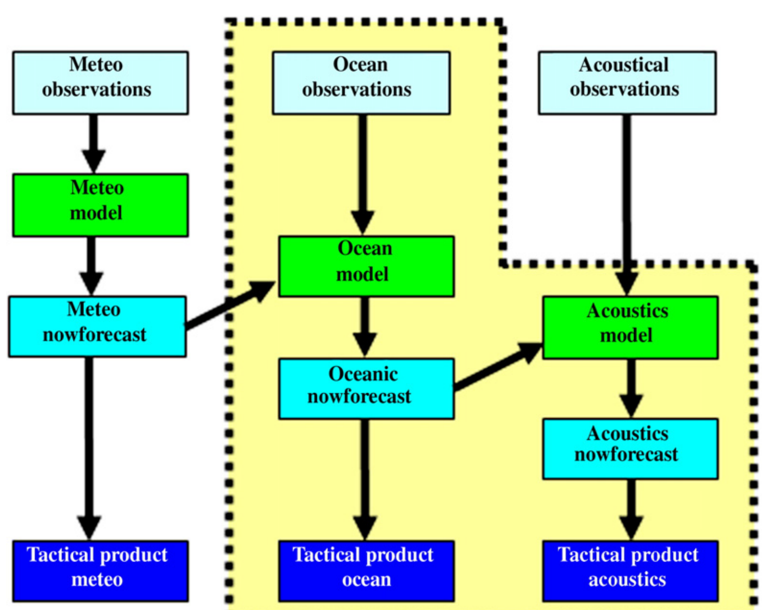

Fig. 6. Process chain starting from observations of meteorology, oceanography, and acoustics, which, using various models, can be used to produce forecasts. These in turn should be converted into tactical products. The activities within the yellow box, performed during NATO/NURC exercise BP07 were performed onboard of HNLMS Snellius and are described in this paper. (For interpretation of the references to colour in this figure legend, the reader is referred to the web version of this article.)

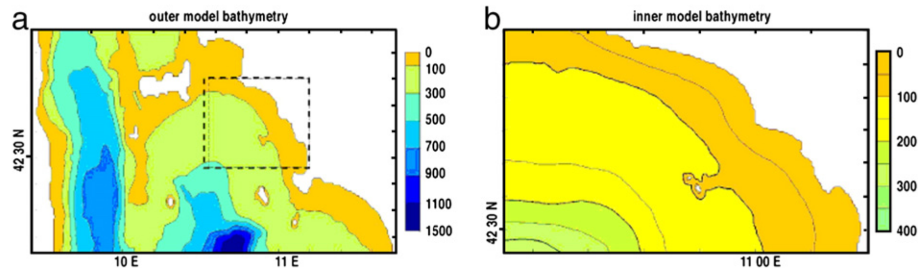

Fig. 7. Bathymetry of the outer (a) and inner (b) model domains. Depths are in meters. Details of the domains are given in Table 1.

is always below the mixed layer depth in the spring situation around Elba. Furthermore, the scenario (Section 4.3) was simplified by using fixed sediment parameters: emphasis is on variability in the water column.

3.2.1. Oceanographic modeling system

The oceanographic modeling system was based on the MIT Multidisciplinary Simulation, Estimation, and Assimilation System (MSEAS). This system includes oceanographic primitive-equation (Haley et al., 1999) and tidal models (Logutov and Lermusiaux, 2008) with data assimilation (Lermusiaux et al., 2002b, 2006a). The primitive-equation model used here was that of the Harvard Ocean Prediction System (HOPS, Robinson et al., 1996; Robinson, 1999). This ocean model was primarily designed for regional applications with modular schemes for rapid set-up, data assimilation and dynamical studies. In addition to topography conditioning software, data processing and gridding routines, initialization and assimilation schemes, dynamical studies schemes, and visualization software, the MSEAS modeling activities now also involve forward and inverse barotropic tidal prediction schemes and multi-scale nested modeling with free-surface ocean models.

For BP07, the ocean simulations were set up over a pair of two-way nested domains, centered on the focal region (Fig. 7). Characteristics of the two domains are given in Table 1. The two nested domains have sigma-levels in the vertical, which makes them appropriate for the region, which is characterized by shallow (<200 m) areas and deep areas further south and west.

The bathymetry and relative positions of the two nested domains are seen in Fig. 7. The outer modeling domain encompassed the full width of the Tyrrhenian Sea between Italy and Sardinia, so as to fully cover the transport through the strait in the west (Corsica Channel), as changes in the larger scale flow through there can affect the focus region of the BP07 exercise.

3.2.2. Initialization and boundary conditions

Within the oceanographic and acoustic forecasting component of the exercise, forecasts for relevant parameters such as full column water temperature, current strength and direction, sound velocity and acoustic propagation losses were provided (see Section 4). To arrive at such forecasts, an initial state is needed, as well as information on the forces driving oceanic variability. To establish an initial state, historical, climatological and synoptic in situ observations as well as remotely sensed observations can be used.

In the Mediterranean, we had found through our exercises (Lermusiaux, 1999b; Robinson, 1999; Coelho et al., 2004; Leslie et al., 2008) that using climatological data sets is not often adequate due to seasonal and longer-time scale changes in the mean ocean fields in the region. Similar findings have been reported by Pinardi and Masetti (2000), Onken et al. (2003, 2008), and others. As a result, the data suitable for initialization included: the in situ observations (Section 3), sea-surface temperature data from satellite observations, and large scale fields from the Mediterranean Forecast System (MFS, Pinardi et al., 2003). The basin-scale MFS model assimilates satellite and in situ observations, and routinely distributes analysis and forecast fields for the Mediterranean. Both the analysis and forecast fields were kindly provided to the BP07 exercise by the MFS consortium. At TNO in The Hague, the MFS forecasts and analyses were downloaded daily and the relevant regions of the data were extracted for transmission to the ship, so as to limit communication needs.

Before and at the start of BP07, the MFS predictions were utilized to initialize our modeling simulations and so provide inputs to the acoustic modeling simulations. Utilizing boundary conditions from a larger scale model (MFS) to the ship given its limited data communication facilities was one of the components we wished to demonstrate. In real-time, this MFS forcing of our local high-resolution model runs was successful from the logistics view point, involving the MFS staff in Bologna, TNO in The Hague, and the operational modeling staff onboard the ship. However, due to rapid localized changes observed in the data, for the operational runs that we issued (and described in this manuscript), we relied solely on in-situ data for the initialization. For open boundary forcing, we utilized open boundary condition schemes (Haley et al., 2009). We did not issue the runs that used real-time MFS for larger-scale boundary forcing (MFS had not assimilated our real-time measurements).

A finding of our exercise (see also Section IV.2) is that the use of the in situ data (Figs. 2b, 3 and 4) was necessary to initialize our model simulation and provide stable and useful acoustic predictions. This is due both to the high-resolution requirements of our ocean–acoustic model simulations and to the difficulty of obtaining accurate predictions of the ocean mean fields in the recently variable Mediterranean climate.

3.2.3. Atmospheric forcing

Atmospheric forcing includes the surface wind stress, which provides an input of momentum in the upper layers of the ocean; and the fluxes of heat and freshwater, resulting mostly from sunshine, precipitation, and evaporation. Forecasts for these quantities were from the French Service Hydrographique et Oceanographique de la Marine (SHOM), based on high-resolution simulations by the ALADIN atmospheric model.

These atmospheric ALADIN fluxes are then interpolated to the ocean model grids. These forecasts were posted almost daily, and provided predictions up to three days ahead. Momentum fluxes from the atmosphere to the ocean in latitudinal and meridional direction, as well as freshwater fluxes (precipitation minus evaporation) were

Table 1
Model domain parameters.

	Outer model	Inner model
Horizontal resolution	900 m	300 m
Number of horizontal grid cells	213 × 106	179 × 126
Longitudinal boundaries	009° 25'–011° 45' E	010° 33'–011° 12' E
Latitudinal boundaries	42° 08'–43° 00' N	42° 28'–42° 48' N
Number of sigma layers	20	20
Mean and median depth	181 m/95 m	88 m/93 m
Deepest depth	1293 m	339 m

directly fed to the forcing interpolation scheme of our primitive-equation model. The total heat flux was evaluated by addition of the ALADIN predictions for sensible and latent heat flux, shortwave and longwave radiation.

In our simulations, a mixing-layer model transfers and dissipates the atmospheric forcing in the oceanic surface boundary layer (for details, see Lermusiaux, 2001). Using the wind-stress computed from ALADIN, it first evaluates a turbulent friction velocity. A local depth of turbulent wind-mixing or Ekman depth is then defined, assuming it is locally linearly proportional to the given turbulent friction velocity and limited by rotation. Once this depth is computed, vertical eddy coefficients within this surface layer are set to empirical values. Presently, these parameters can be optimized based on the observed mixed-layer and the atmospheric forcing.

3.2.4. Data assimilation and data collection using model guidance

The assimilation of in situ observations during our simulations was carried out by Optimal Interpolation (Lozano et al., 1996; Lermusiaux, 1999a). Data are first gridded (objectively analyzed) onto the model grid, depth-by-depth, which ultimately results in a full three-dimensional field. To do so, decorrelation scales of 1 day in time and 10 km in space were used. To evaluate the coverage of the data, error maps are computed for each gridded data field. Gridded data and model fields are then blended in accord with these error-maps: where the data error is low, the value predicted by the model is substantially updated by the data and vice versa. The gridded data fields are here temperature and salinity fields. Geostrophic velocity shear is computed from these hydrographic fields and used to correct the corresponding velocities of the model forecast. As a whole, the correction added to the model forecast at data times is in dynamical balance, within specified error bounds of the hydrographic data and of the assumption of geostrophic balance for the vertical velocity shear associated with this data.

Our ocean forecasting began upon the acquisition of a minimal initialization dataset. As forecasting runs are much improved by assimilating recent observations, we continued to sample whenever the ship schedule permitted. A first set of homogeneously (in space) and synoptically (in time) sampled data in the vicinity of the focal region of the exercise was acquired between late April 29 and April 30 (Fig. 8, third panel). This dataset was then assimilated into the model as a first "new data". The next night, April 30–May 1, a second assimilation dataset was sampled (Fig. 9, left panel). This dataset focused on the region closest to the land, as our recommendations and that of other MREA07-BP07 models suggested the relative importance of this region to the general flow in the region (Rixen and Coelho, personal communication). On May 2, a third, smaller, dataset was sampled in close proximity to the 100 m depth contour that was central to the acoustics component of the exercise (Fig. 9, central panel). On the last active days of the exercise, a final validation dataset was sampled by the combined efforts of the HNLMS Snellius and the Italian Navy vessel Aretusa (Fig. 9, right panel).

Note that in our model simulations, runs are always re-started in the past so as to assimilate the most recently available data and thus issue the most up to date nowcast and forecast as possible. Typically, the ocean model has at least ran a few hours before the first assimilation data are smoothly entered into the assimilation to reduce shock-effects. The ramp up time of the assimilation data was here set at 6 h. These ocean nowcasts and forecasts are then used as inputs to the acoustic models.

3.2.5. Acoustic modeling coupled to oceanographic modeling

We carried out acoustic modeling with the TNO sonar performance prediction package ALMOST. ALMOST is a range dependent ray tracing sonar performance model. It is developed for the Royal Netherlands Navy and contains modules for the calculation of transmission loss and passive and active sonar range predictions (Schippers, 1995; Etter, 2001). ALMOST can be applied to a wide range of sonar systems, and takes sound speed and bathymetric data as inputs, as well as sediment type.

To carry out the acoustic predictions, the ocean model sound-speed forecasts are interpolated onto a suitable grid for the acoustic modeling. Care is required in doing so in order to account for the possible bathymetric uncertainties as well as other errors arising in the interpolation process. Usually, a vertical interpolation is needed

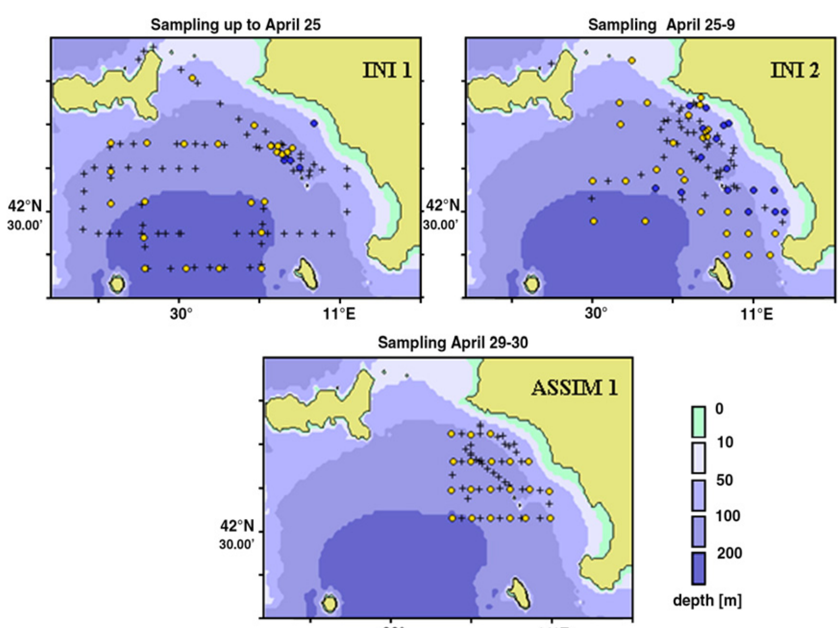

Fig. 8. Initialization dataset (upper two panels INI1 and INI2) and first assimilation dataset (lower panel, ASSIM 1). The circular dots denote CTD stations taken by the two ships (color coded orange for Snellius, and blue for Leonardo). Temperature profiles obtained by the moving vessel profiler (MVP) onboard Snellius are indicated by a '+' sign. The bottom topography is indicated by the shading and contours at 10, 50, 100 and 200 m depth. (For interpretation of the references to colour in this figure legend, the reader is referred to the web version of this article.)

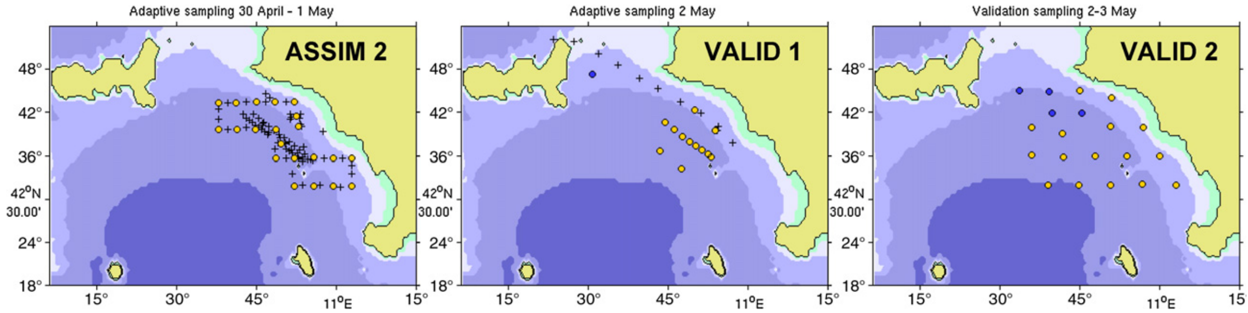

Fig. 9. As Fig. 8, but for the second assimilation (ASSIM 2) and validation/verification datasets (VALID 1 and 2). Blue dots here represent CTD stations gathered by the Italian Navy vessel Aretusa. (For interpretation of the references to colour in this figure legend, the reader is referred to the web version of this article.)

prior to the horizontal one. Once the sound-speed field is mapped to the acoustic grid, a set of acoustic propagation predictions was calculated, reflecting the various acoustic parameters, bearing and source-receiver properties (depths, locations, etc). Such computations were computed every day of the trial, using the latest data-assimilative ocean nowcast and forecasts.

4. Discussions and real-time results

4.1. Atmospheric forcing discussion and results

On a daily basis, the ALADIN high resolution meteorological forecasts for the subsequent days were transferred to the ship. At the beginning of the exercise, we provided routine plots of the surface wind fields from these weather forecasts to the other parties on board. The wind forecasts would then be used to plan some of the acoustical activities, and the initial locations of freely drifting devices.

We found that the daytime Aladin fluxes for hindcast runs are somewhat better temporally resolved than the nighttime fluxes. The Aladin forecasts start at 07:00 h, and for the first 12 h hourly fields are provided (until 18:00 h). From there on, three day forecasts were provided with three hour intervals (21:00 h, 00:00 h, etc.; all times are denoted here in UTC). For hindcast runs, we added the most recent estimates, resulting in higher daytime resolution. An example of these fluxes for the one-week initialization run is given in Fig. 10. While the coarser nighttime resolution appears justified for the net heat flux, the other fluxes may be under-sampled. It should be noted that the meteorological flux forecasts were provided by SHOM in an integrated three-hourly form. The exact timing of maxima and minima may be somewhat displaced, but the integrated fluxes contain the full resolution of the real-time meteorological model. Our ocean model used three-hourly forcing fields, but in a linearly interpolated form between 3-hour periods, so as to ensure a smooth development of the daily forcing cycle.

One notices the (on average) positive heat flux (warming of the sea surface). Over the one week period depicted here, a simple integration of this heat flux into a mixed layer of 5 m thick yields a temperature rise of 1.2 °C. For a thinner three meter thick mixed layer, this temperature rise is higher, up to almost 2 °C. When the mixed layer is thin as in BP07, the parameters in the representation of its dynamics have to be carefully chosen in order to properly forecast surface temperatures.

4.2. Downscaling discussion and results

During the initialization survey we compared the in situ data with the MFS fields we were planning to use. We found a significant mismatch between the observed temperatures and those modeled by the MFS. In Fig. 11, we compare: MFS climatology; a local observations-based climatology for the Mediterranean (MEDAR); and, mean data collected in the first week of the BP07 exercise. Clearly, the data indicate much warmer temperatures (>2° at 50 m) over the upper 100 m of the water column. The two model curves indicate that the MFS-based results for this period are slightly warmer than climatology

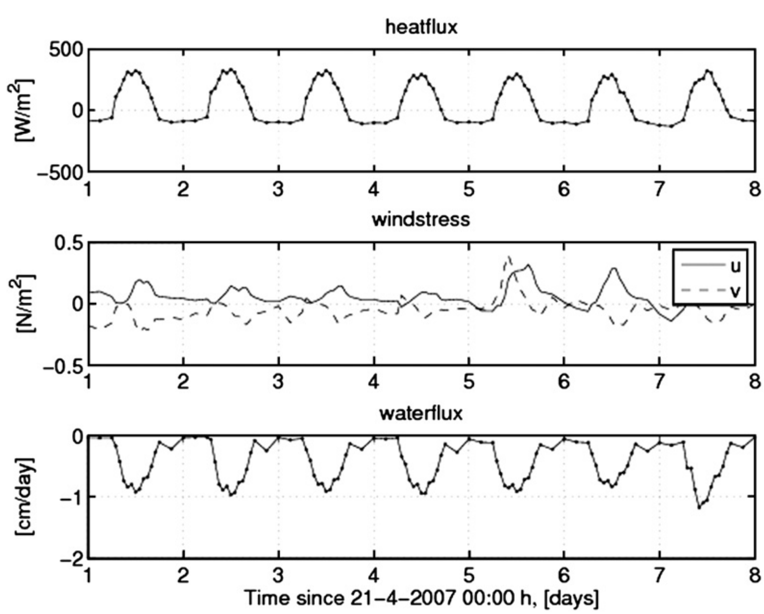

Fig. 10. Fluxes for heat, momentum (both directions) and freshwater for the first week of BP07.

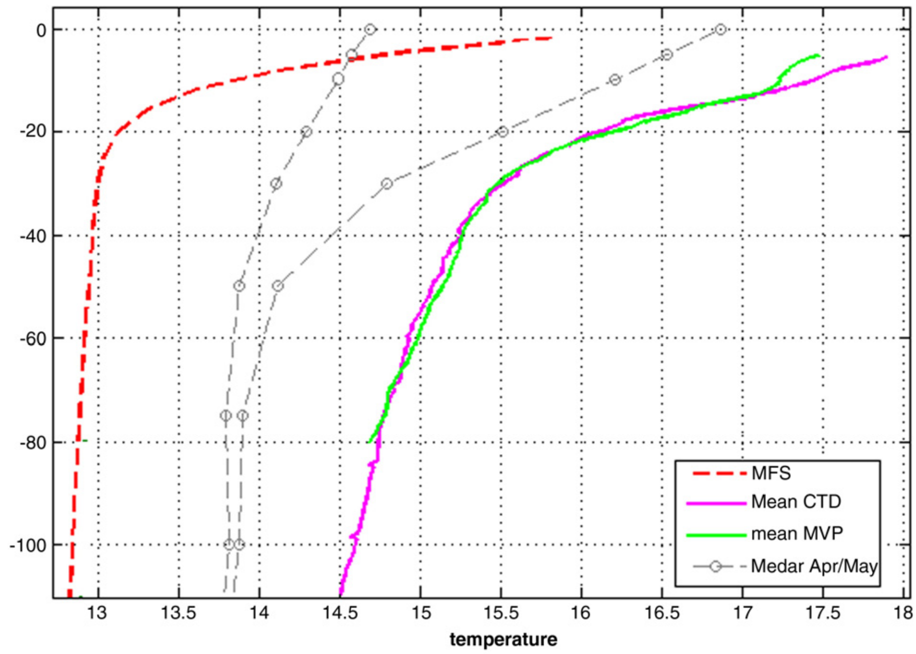

Fig. 11. Comparison of temperature profiles from the MFS model, the MEDAR climatology, and the observations made during the initialization period of BP07.

(for the month of April), but are still considerably cooler than observed. The MEDAR climatologies for April and May are somewhat in between, but are also about 1° cooler than observed. It was concluded from these analyses that further merging of in situ and historical data would not provide a reliable initialization dataset for the period of the BP07 exercise. We therefore used only the in situ data collected during the exercise itself, thereby accepting the lack of resolution and spatial coverage outside of the immediate vicinity of the focus region of the acoustical measurements.

It is important to note that such mismatch between synoptic and climatological data are now frequent in the Mediterranean as we have mentioned above (Section 3.2.2). We have found this to be especially true in the Tyrrhenian basin east of Corsica and Sardinia (during ASCOT-02 and MREA03). We also know of at least one reference to similar discrepancies in the Balearic Sea (Onken et al., 2008). This is one of the main reasons why the downscaling of basin-scale models assimilating a limited number of ocean data is challenging in the region. The utilization of local synoptic data is recommended whenever available.

4.3. Real-time coupled oceanographic–acoustic forecasts discussion and results

As soon as the initialization campaign was completed, we began ocean forecasts based on the available initial data and the meteorological forecasts. Fig. 12 provides a schematic description of the schedule of observations, model runs, and acoustic forecasts. Forecasts follow the 8-day long initialization run. Two of these forecast runs are discussed here, each with different sets of assimilation data. As indicated on Fig. 12, the last sets of observations were not available for use in real-time, neither for assimilation nor validation. A hindcast run utilizing all three assimilation datasets is envisioned for the near future. As a preliminary validation based on the runs performed in real-time, we compared the first validation dataset (which was acquired on May 2) to the model predictions issued May 1. In Fig. 13, we show the root mean square (RMS) difference in temperature between the modeled forecast and measured CTD stations (solid line). To estimate model forecast skill, we may compare this data-forecast

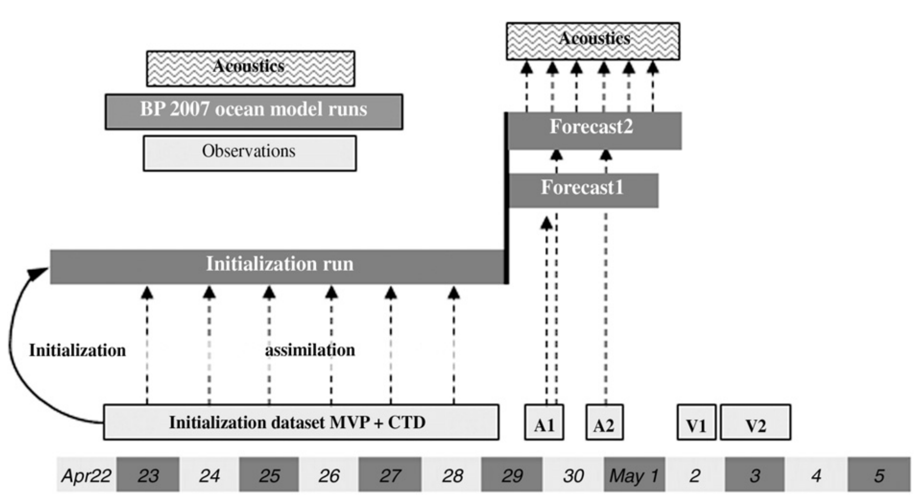

Fig. 12. Along the horizontal axis in this schematic is the timeline of the BP07 exercise. Above it, the different layers of activities are drawn, with the observational level, the oceanographic modeling levels, and the acoustic forecasting level on top. Assimilation datasets are denoted A1 and A2, validation datasets by V1 and V2 (see Figs. 8 and 9).

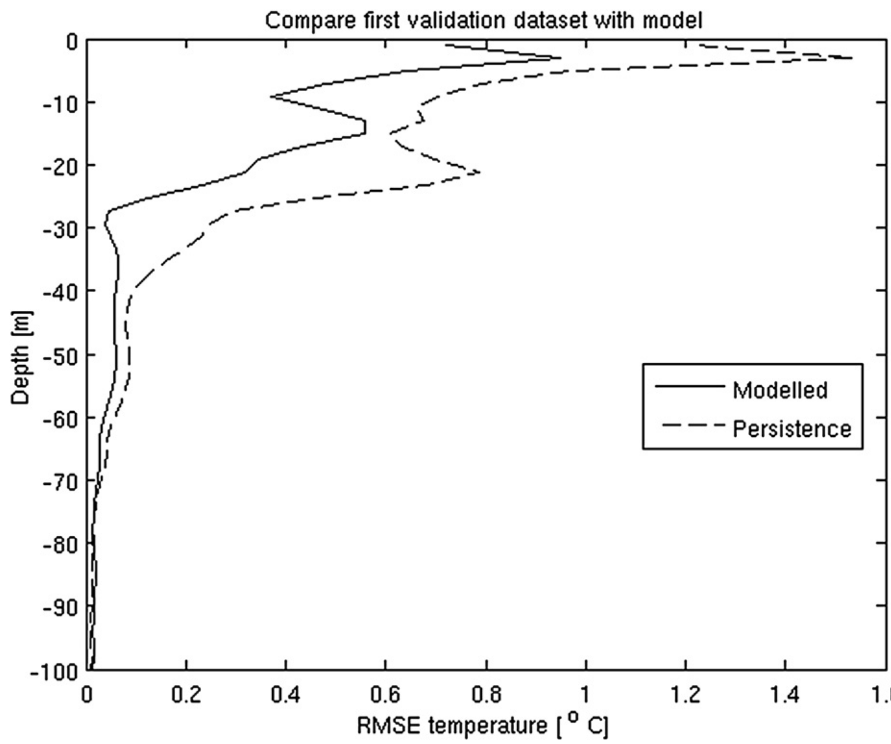

Fig. 13. The root mean square error of observations from the first validation dataset, compared to the model forecast for May 1 (solid line) and persistence (dashed line). A reduction of the error indicates that at those levels, the model forecast is better than a persistence scenario, i.e. the ocean tomorrow is the same as the ocean today.

RMS difference to the RMS difference between the observations and a 'persistence' scenario, in which the model is not used, and its initial conditions are presumed steady (dashed line). This skill assessment gives us some confidence that the real-time ocean model predictions had some predictive capability.

From the forecast runs, three-hourly states were saved and various plots were routinely created, compiled in a web-based structure and made available to the other exercise members via the internet. For each forecast, surface velocity vectors were shown on two scales (Fig. 14), zooming in on the focal line of the acoustics component of the exercise (red line in Fig. 14a and b). These surface flow fields were then used (in combination with the meteorological forecasts) for planning purposes mostly for the freely drifting acoustic devices.

From the ocean forecasts of temperature and salinity, sound velocity was computed using the UNESCO 1983 polynomial (Fofonoff and Millard, 1983). The focus of the acoustics campaign was on a 15 km long transect following the 110 m isobath southeast of Elba island and we routinely provided section plots of temperature and sound velocity forecasts along this line.

In the last week of the exercise, the primitive-equation ocean forecasts were coupled to the Acoustic Loss Model for Operational Studies and Tasks (ALMOST) acoustical performance prediction toolbox, to create estimates of the detection probability in the given ASW scenario. The ALMOST sonar performance prediction tool uses eigenrays to compute reverberation levels and transmission losses for a particular scenario of transmitter and target specifics, noise levels and background configuration. From the transmission losses and reverberation levels,

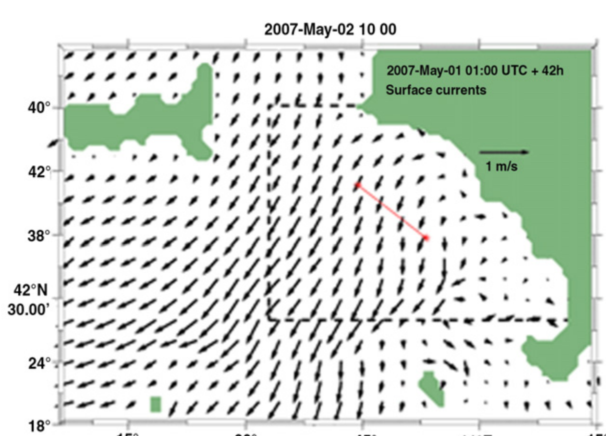

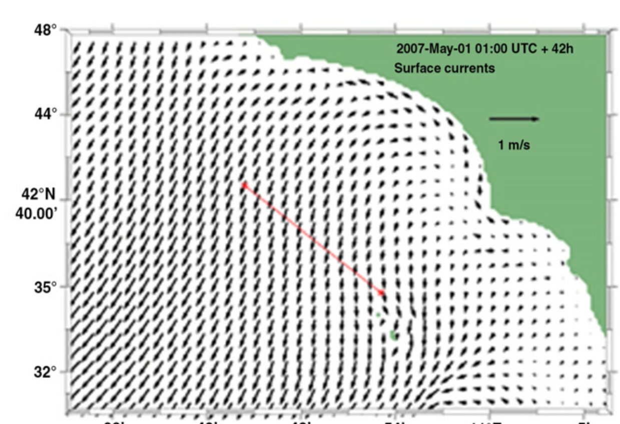

Fig. 14. (Left) The surface current forecast of our primitive-equation ocean model for the outer model domain. The dashed rectangle denotes the region of the smaller domain, higher resolution model. (Right) Surface current forecast for the inner model.

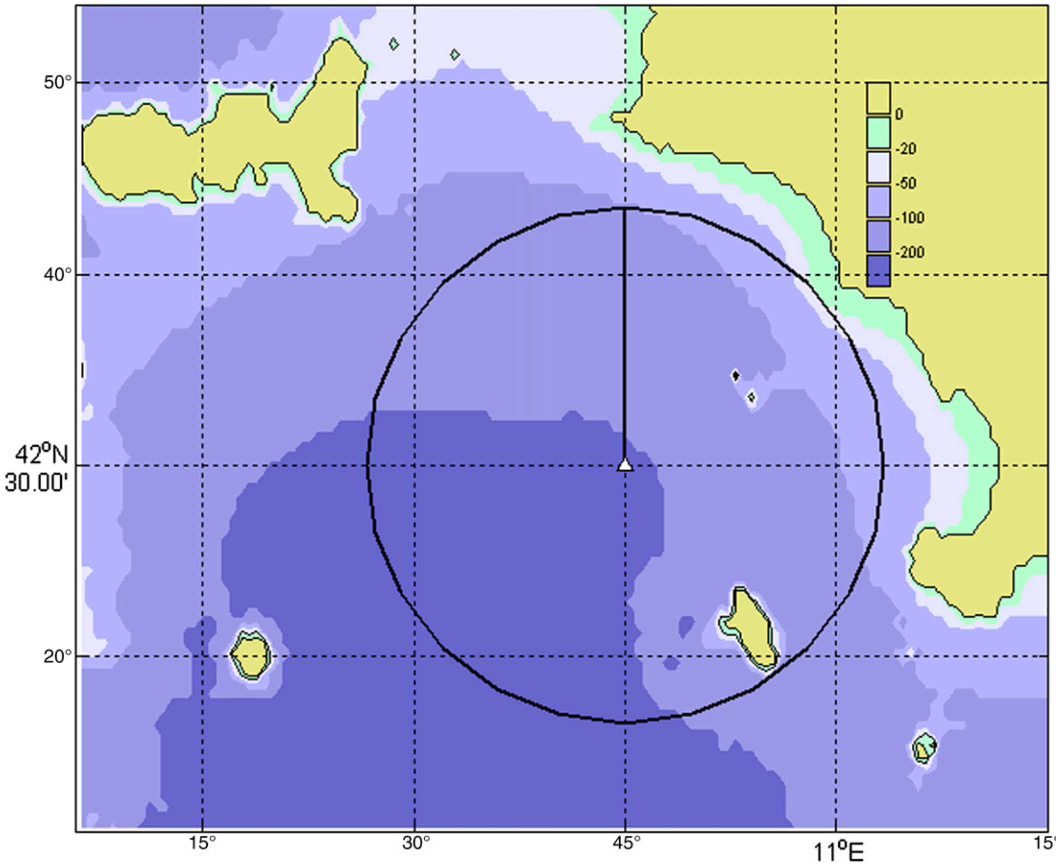

Fig. 15. Region for the acoustics evaluation, with the black circle representing the area of a sonar image of a ship traveling Northward, which was the scenario used for our ALMOST computations.

ALMOST calculates a probability of detection (PoD) between 0 (no detection capability) and 1 (certain detection). The scenario used for the acoustics prediction was based on a moderate low frequency active sonar (LFAS), being towed by a ship positioned at 42°30′N, 10°45′E, heading north; the situation is shown in Fig. 15.

The ALMOST scenario parameters are given in Table 2. As ALMOST is a two-dimensional model, for each ocean forecast, we did 24 runs with 25 km long sections starting at the ship position. From these sections, a complete picture of the detection probability for the circular region centered at this location (as shown in Fig. 15) can be drawn. This region comprises most of the area covered during the exercise, as well as depths between at most 50 m near the coast, and over 500 m in the southwestern part of the 25 km radius circle around the ship.

ALMOST calculations were made based on MSEAS predictions at a number of 12 hour-intervals after the initial estimates of April 30th at 19:00 (nowcast). Examples of the temperature and sound speed nowcast and forecasts are shown in Figs. 16 and 17, respectively. The main variations in temperature and sound speed occur in and above the thermocline at larger ranges (>10 km).

The propagation loss computed with ALMOST (Fig. 18) shows the effect of the ocean variability. With the 12 h forecast, which has a weaker vertical gradient in sound speed at large ranges, the propagation loss at ranges beyond 17 km has decreased compared to the nowcast, whereas in the 36 h forecast (with a stronger sound speed gradient) it has increased.

The calculated PoD for the circular region based on these nowcast and forecasts is shown in Fig. 19. Black colors denote regions of low detection probability, the crosses in the plots show the heading of the ship, and illustrate the spacing between the values of bottom depth used. The ocean variability also influences the PoD: in the direction along which the sections in Figs. 16–18 were taken (indicated by the green star) the PoD is largest for the 12 h forecast, which had the least propagation loss at large ranges. In general, the ocean variability is found to influence the detection probability considerably, especially in the shallower areas towards the east. This is due to the updated observations, atmospheric forcing variability and (sub)-mesoscale ocean conditions observed in the near shore area over this 24 h period. Also, the probability of detection of a submarine at closer ranges towards the west and southwest are found to be strongly reduced over the period of the forecast. We expect that the warming of ocean

Table 2
ALMOST scenario parameters.

Parameter	Value
Setup	
Towed body source (horizontally omni-directional);	2 free flooded rings (FFRs)
Source level	220 dB re 1 μPa at 1 m
Central frequency	1500 Hz
Pulses	2 s FM , bandwidth of 600 Hz
Towed receiving array	96 elements
Left-right ambiguity resolved	Yes
Operation depth (source and receiver)	50 m
Tow ship noise (taken at 200 m distance)	Spectral level 116 dB/Hz
Detection threshold (for each beam)	Based on Prob. of false alarm of pfa = 1.e-05
Target depth/target strength	50 m/10 dB
Range of computational domain	25 km
Environment	
Sound velocity/bathymetry	From MSEAS ocean forecasts/grid
Absorption module	Francois-Garrison, pH = 7.9
Sediment	Clay

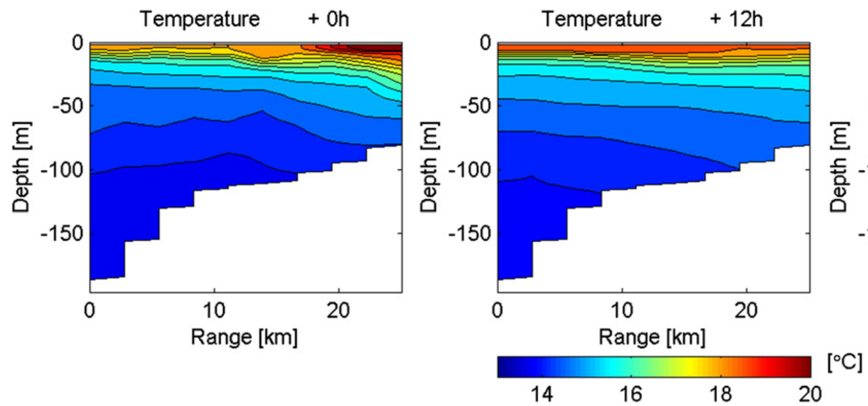

Fig. 16. Temperature nowcast and forecast examples. The nowcast (left) is for April 30, 19:00 h, the forecasts for 12 h (middle) and 36 h (right) later. The section is taken from the center of the acoustics evaluation region shown in Fig. 15 in east-southeasterly direction (see also Fig. 19).

surface layers in these regions, as well as inflows into the acoustic domain of interest is responsible for these differences. Even though the ocean data for validation is limited, the final hindcast simulations should shed some more light on these processes responsible for the variability of the predicted acoustic performance.

5. Conclusions and recommendations

For BP07, we have set-up the complete chain of operational oceanographic–acoustic forecasting, from using meteo fields, collecting in situ measurements and data assimilation to the provision of tactical data in the form of acoustic forecasts. This operational system had two components: an at-sea modeling capability for rapid coupled ocean–acoustic predictions and onshore support for data quality control and management, scientific and computational guidance. On a regular basis, questions, discussions and datasets were exchanged between the Mediterranean Sea and the MIT-Boston based MSEAS team. It is important to note that, to our knowledge, this joint effort is the first time that range and bearing dependent acoustic performance predictions coupled to data-assimilative oceanographic forecasts were carried out at sea, in real-time. Previously, at least one of these computations was run ashore.

Importantly, the effort here was to evaluate the feasibility of collaborating in real-time with a scientific research team to carry out operational system research at sea. Demonstrating that such coupled ocean–acoustic predictions could be issued at sea was an objective more important than evaluating the details of the predictions. However, a thorough investigation of the predictions and their relation to

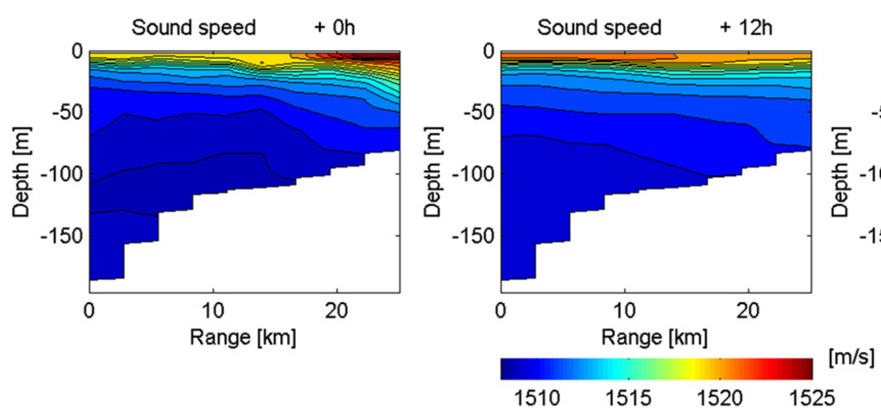

Fig. 17. As Fig. 16, but for sound speed.

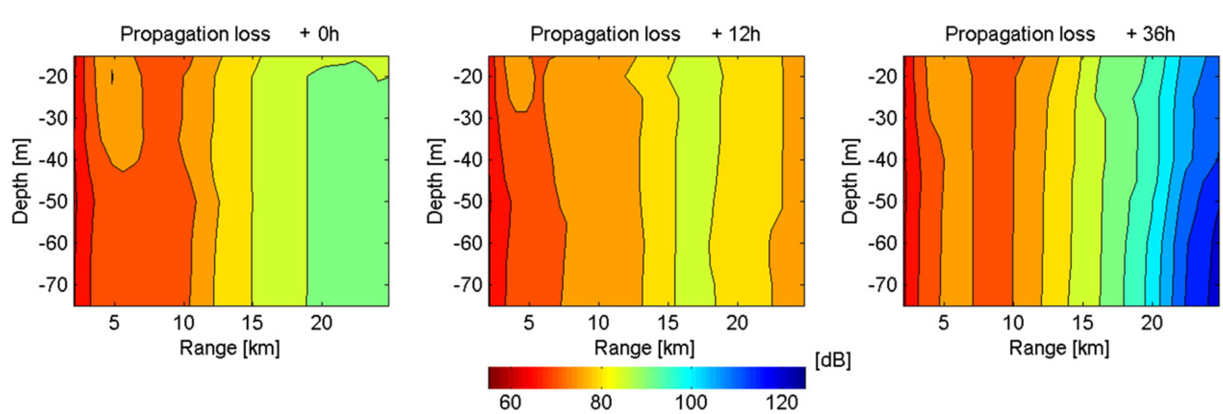

Fig. 18. Propagation loss computed with the ALMOST acoustics tool along the same section as the temperature and sound speed examples shown in Figs. 16 and 17.

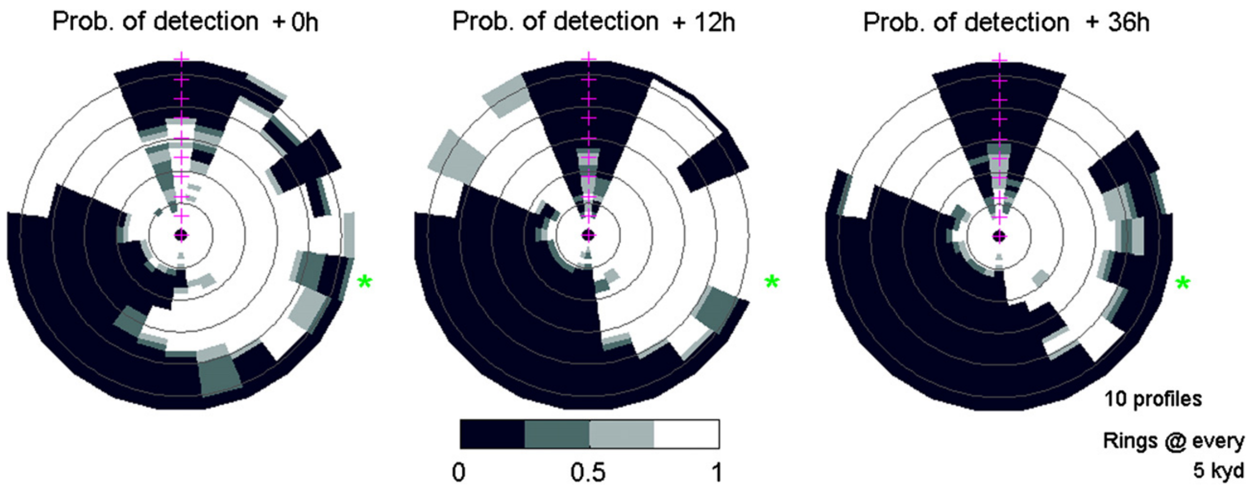

Fig. 19. Probability of detection nowcast and forecast examples for the region shown in Fig. 15 and for the ASW scenario summarized in Table 2. The green star indicates the direction of the beam along which the sections in Figs. 16–18 were taken. (For interpretation of the references to colour in this figure legend, the reader is referred to the web version of this article.)

the observed validation physical and acoustic data is a necessary next step for the near future. This will be carried out once the acoustic data has been analyzed and filtered by our BP07 colleagues.

We experienced that the downscaling of basin-scale models assimilating a limited number of ocean data is challenging in the region. The utilization of local synoptic data is recommended whenever available. We also found that simply using a fixed or climatological ocean estimate in the Mediterranean Sea for acoustic propagation prediction is not likely to lead accurate results anymore. This is likely due to natural changes occurring in the Mediterranean but also to human activities and global climate changes.

The link between the oceanographic and acoustic modeling components was shown to be important. This observation can be expected to have significant impact on future activities in the Mediterranean Sea, most notably on naval operations such as acoustic surveillance but also on acoustic–oceanographic scientific studies. Even in this relatively quiet region around Elba, the oceanographic variability seemed to have had a profound influence on the acoustical propagation properties, and thereby on the tactical level of submarine detectability. Of course, we only tested a relatively shallow submarine scenario. For somewhat deeper transmitters and receivers, the results may not be as sensitive to local ocean variability. However, the closer to the surface a submarine is located, the more important mixed layer and frontal dynamics effects may become.

Once set up properly, the MSEAS software system was found to be robust, flexible and running swiftly enough to be able to provide timely forecasts, including the use of the available measurements and forcing fields. A certain level of experience in tuning many of the parameters, in making the right choices for initialization, assimilation and validation is required, and substantial training was provided.

For future research, the process of setting up and tuning of complex ocean prediction systems for a specific location could be further streamlined. For example, if one was able to automatically setup new model domains, grids and initialization fields, all at once, including automatic checks of software, compiler options and numerical and physical parameters, one could then directly and rapidly adapt to changes in the observational campaign, without support from onshore experts. Work has been carried out along these directions (e.g. Evangelinos et al., 2006), but much applied system research remains for these distributed and automated control of complex software systems. In addition to coupling the oceanographic–acoustic modeling, the data assimilation process can also be coupled, merging acoustic (Elisseeff et al., 2002) and oceanographic data assimilation (Robinson and Lermusiaux, 2001; Lermusiaux et al., 2006b) into coupled oceanographic–acoustic data assimilation (Lermusiaux and Chiu, 2002; Lermusiaux et al., 2002a). Such coupled assimilation and coupled realistic modeling has not yet been carried out in real-time at-sea but research is underway. A last area of research is to provide adaptive sampling recommendations (Heaney et al., 2007; Yilmaz et al., 2008; Wang et al., 2009-this volume) in real-time that are directly based on coupled acoustic–oceanographic forecasts, aiming to measure the environmental properties and acoustic characteristics that are most relevant for acoustic surveillance and detections.

Acknowledgements

We thank all of our MREA colleagues and collaborators without which the BP07 exercise would not have been possible. Specifically, we thank Dr. Hermand and LeGac for their role in the organisation. We also thank Dr. Coelho (NRL-Stennis), Dr. Logutov (MIT) and the captain and crew of the HNLMS Snellius for their inputs during the exercise, as well as the NLHO for their support and preparations. We are grateful to the French Service Hydrographique et Oceanographique de la Marine (SHOM) for their atmospheric forcing fields (ALADIN) and to the Mediterranean Forecast System team for their basin-scale Mediterranean ocean forecasts. Vincent Newsum (TNO) assisted with the extraction of MFS data files. PFJL, PJH and WGL gratefully thank the Office of Naval Research for research support under grant PLUSNet (S05-06), ONR6.1 (N00014-07-1-1061), ASRTP (N00014-07-1-0534) and PLUS-INP (N00014-08-1-0680) to the Massachusetts Institute of Technology. TNO funding was supplied by the Defense Materiel Organisation, supervised by LCDR René Dekeling, who also assisted with the communication lines on board HNLMS Snellius. We thank the (anonymous) reviewers for their valuable comments that were of great help in improving this manuscript.

References

Abbot, P., Dyer, I., 2002. Sonar performance predictions based on environmental variability. In: Pace, N.G., Jensen, F.B. (Eds.), Acoustic Variability, 2002, pp. 611–618. SACLANTCEN. Kluwer.

Allard, R., Dykes, J., Hsu, Y.L., Kaihatu, J., Conley, D., 2008. A real-time nearshore wave and current prediction system. J. Mar. Syst. 69 (1–2), 37–58.

André, G., Garreau, P., Garnier, V., Fraunié, P., 2005. Modelled variability of the sea surface circulation in the North-western Mediterranean Sea and in the Gulf of Lions. Ocean Dynamics 55 (3–4), 294–308. doi:10.1007/s10236-005-0013-6.

Artale, V., Astraldi, M., Buffoni, G., Gasparini, G.P., 1994. The seasonal variability of the gyre-Scale circulation in the northern Tyrrhenian Sea. J. Geophys. Res. 99, 14,127–14,137.

Astraldi, M., Gasparini, G.P., 1992. The seasonal characteristics of the circulation in the north Mediterranean Basin and their relationship with the atmospheric-climatic conditions. J. Geophys. Res. 97 (C6), 9531–9540.

Astraldi, M., Gasparini, G.P., 1994. The seasonal characteristics of the circulation in the Tyrrhenian Sea. In: La Violette, P.E. (Ed.), The seasonal and interannual variability of the western Mediterranean Sea. Coastal and Estuarine Studies, vol. 46. AGU, Washington, pp. 115–134.

Astraldi, M., Gasparini, G.P., Vetrano, A., Vignudelli, S., 2002. Hydrographic characteristics and interannual variability of water masses in the central Mediterranean: a sensitivity test for long-term changes in the Mediterranean Sea. Deep-Sea Res. I 49, 661.

Carriere, O., Hermand, J.-P., Le Gac, J.-C., Rixen, M., 2009. Full field tomography and Kalman tracking of the range-dependent sound speed field in a coastal water environment. J. Mar. Sys. 78, S382–S392 (this issue).

Coelho, E.F., Robinson, A.R., 2003. NATO tactical ocean modeling: the mini-HOPS strategy in the Maritime Rapid Environmental Assessment 2003 Sea Trial. MREP03 Proceedings, NATO Undersea Research Centre CP-47/CD-70.

Coelho, E.F., Rixen, M., 2008. Maritime rapid environmental assessment new trends in operational oceanography. J. Mar. Syst. 69, 1–2.

Coelho, E.F., Rixen, M., Signell, R., 2004. NATO tactical ocean modeling system: concept applicability, NATO Undersea Research Centre Serial Report, SR-411.

Elisseeff, P., Schmidt, H., Xu, W., 2002. Ocean acoustic tomography as a data assimilation problem. IEEE J. Oceanic Eng. 27, 275–282.

Etter, P.C., 2001. Recent advances in underwater acoustic modeling and simulation. J. Sound Vibration 351–383.

Evangelinos, C., Lermusiaux, P.F.J., Geiger, S., Chang, R.C., Patrikalakis, N.M., 2006. Web-enabled configuration and control of legacy codes: an application to ocean modeling. Ocean Model. 13, 197–220.

Fofonoff, P., Millard, R.C. Jr., 1983. Algorithms for computation of fundamental properties of seawater, 1983. Unesco Tech. Pap. in Mar. Sci., No. 44, 53 pp.

Gasparini, G.P., Ortona, A., Budillon, G., Astraldi, M., Sansone, E., 2005. The effect of the Eastern Mediterranean Transient on the hydrographic characteristics in the Strait of Sicily and in the Tyrrhenian Sea. Deep-Sea Res. I 52, 915–935.

Gerkema, T., Lam, F.P.A., Maas, L.R.M., 2004. Internal tides in the Bay of Biscay: conversion rates and seasonal effects. Deep-Sea Res. II 51, 2995–3008.

Haley, P.J., Lermusiaux, P.F.J., Leslie, W.G., Robinson, A.R., 1999. Harvard Ocean Prediction System (HOPS). http://mseas.mit.edu/HOPS.

Haley, P.J. Jr., Lermusiaux, P.F.J., Robinson, A.R., Leslie, W.G., Logutov, O., Cossarini, G., Liang, X.S., Moreno, P., Ramp, S.R., Doyle, J.D., Bellingham, J., Chavez, F., Johnston, S., 2009. Forecasting and Reanalysis in the Monterey Bay/California Current Region for the Autonomous Ocean Sampling Network-II Experiment. Special issue on AOSN-II. Deep Sea Research, Part II 56, 127–148 ISSN 0967-0645.

Heaney, K.D., Gawarkiewicz, G., Duda, T.F., Lermusiaux, P.F.J., 2007. Non-linear optimization of autonomous undersea vehicle sampling strategies for oceanographic data-assimilation. special issue on "underwater robotics". J. Field Robotics 24 (6), 437–448.

Kalman, R.E., 1960. A new approach to linear filtering and prediction problems. Trans. ASME – J. Basic Eng. 82, 35–45.

Kirwan Jr., A.D., Robinson, A.R., 1997. Assimilation and modeling, executive summary in rapid environmental assessment. In: Pouliquen, E., KirwanJr. Jr., A.D., Pearson, R.T. (Eds.), SACLANTCEN Conference Proceedings Series CP-44, pp. x–xi.

Ko, D.S., Martin, P.J., Rowley, C.D., Preller, R.H., 2008. A real-time coastal ocean prediction experiment for MREA04. J. Mar. Syst. 69, 17–28.

Lam, F.P.A., Maas, L.R.M., Gerkema, T., 2004. Spatial structure of tidal and residual currents as observed over the shelf break in the Bay of Biscay. Deep-SeaRes. I 51, 1075–1096.

Lermusiaux, P.F.J., 1999a. Data assimilation via error subspace statistical estimation. Part II: Middle Atlantic Bight shelfbreak front simulations and ESSE validation. Mon. Weather Rev. 127 (7), 1408–1432.

Lermusiaux, P.F.J., 1999b. Estimation and study of mesoscale variability in the Strait of Sicily. Dyn. Atmos. Ocean. 29, 255–303.

Lermusiaux, P.F.J., 2001. Evolving the subspace of the three-dimensional multiscale ocean variability: Massachusetts Bay. J. Mar. Syst. 29/1–4, 385–422. Special issue on "Three-dimensional ocean circulation: Lagrangian measurements and diagnostic analyses.

Lermusiaux, P.F.J., 2007. Adaptive modeling, adaptive data assimilation and adaptive sampling. In: Jones, C.K.R.T., Ide, K. (Eds.), Special issue on "Mathematical Issues and Challenges in Data Assimilation for Geophysical Systems: Interdisciplinary Perspectives". Physica D, vol. 230, pp. 172–196.

Lermusiaux, P.F.J., Robinson, A.R., 2001. Features of dominant mesoscale variability, circulation patterns and dynamics in the Strait of Sicily. Deep Sea Res. 48 (9), 1953–1997.

Lermusiaux, P.F.J., Chiu, C.-S., 2002. Four-dimensional data assimilation for coupled physical-acoustical fields (.pdf). In: Pace, N.G., Jensen, F.B. (Eds.), Acoustic Variability, 2002. SACLANTCEN. Kluwer Academic Press, pp. 417–424.

Lermusiaux, P.F.J., Chiu, C.-S., Robinson, A.R., 2002a. Modeling uncertainties in the prediction of the acoustic wavefield in a shelfbreak environment. Proceedings of the 5th ICTCA, May 21–25, 2001, in Theoretical and Computational Acoustics 2001, E.-C. Shang, Q. Li, T.F. Gao (Eds.), World Scientific Publishing Co., 191–200.

Lermusiaux, P.F.J., Robinson, A.R., Haley Jr., P.J., Leslie, W.G., 2002b. Advanced interdisciplinary data assimilation: filtering and smoothing via error subspace statistical estimation. Proceedings of Oceans 2002 IEEE/MITS Conference, pp. 795–802.

Lermusiaux, P.F.J., Chiu, C.-S., Gawarkiewicz, G.G., Abbot, P., Robinson, A.R., Miller, R.N., Haley, P.J., Leslie, W.G., Majumdar, S.J., Pang, A., Lekien, F., 2006a. Quantifying uncertainties in ocean predictions. In: Paluszkiewicz, T., Harper, S. (Eds.), Oceanography, Special issue on "Advances in Computational Oceanography", vol. 19, 1. pp. 92–105.

Lermusiaux, P.F.J., Malanotte-Rizzoli, P., Stammer, D., Carton, J., Cummings, J., Moore, A.M., 2006b. "Progress and prospects of U.S. data assimilation in ocean research". In: Paluszkiewicz, T., Harper, S. (Eds.), Oceanography, Special issue on "Advances in Computational Oceanography", vol. 19, 1, pp. 172–183.

Leslie, W.G., Robinson, A.R., Haley Jr., P.J., Logutov, O., Moreno, P.A., Lermusiaux, P.F.J., Coelho, E., 2008. Verification and training of real-time forecasting of multi-scale ocean dynamics for maritime rapid environmental assessment. J. Mar. Syst. 69, 3–16.

Logutov, O.G., Robinson, A.R., 2005. Multi-model fusion and error parameter estimation. QJRMS 131, 3397–3408.

Logutov, O.G., Lermusiaux, P.F.J., 2008. Inverse barotropic tidal estimation for regional ocean applications. Ocean Model 25, 17–34. doi:10.1016/j.ocemod.2008.06.004.

Lozano, C.J., Robinson, A.R., Arango, H.G., Gangopadhyay, A., Sloan, Q., Haley, P.J., Anderson, L., Leslie, W.G., 1996. An interdisciplinary ocean prediction system: assimilation strategies and structured data models. In: Malanotte-Rizzoli, P. (Ed.), "Modern Approaches to Data Assimilation in Ocean Modeling". Elsevier Science, pp. 377–410.

Lynch, J.F., Gawarkiewicz, G.G., Chiu, C.-S., Pickart, R., Miller, J.H., Smith, K.B., Robinson, A.R., Brink, K., Beardsley, R., Sperry, B., Potty, G., 1997. Shelfbreak PRIMER – an integrated acoustic and oceanographic field study in the mid-Atlantic Bight. In: Zhang, R., Zhou, J. (Eds.), Shallow-Water Acoustics. China Ocean Press, pp. 205–212.

Maas, L.R.M., Benielli, D., Sommeria, J., Lam, F.P.A., 1997. Observation of an internal wave attractor in a confined, stably stratified fluid. Nature 388 (6642), 557–561.

Millot, C., 1999. Circulation in the Western Mediterranean Sea. J. Mar. Syst. 20 (1–4), 423–442.

Onken, R., Robinson, A.R., Lermusiaux, P.F.J., Haley Jr., P.J., Anderson, L.A., 2003. Data driven simulations of synoptic circulation and transports in the Tunisia–Sardinia–Sicily region. J. Geophys. Res. 108 (C9), 8123–8136.

Onken, R., Robinson, A.R., Kantha, L., Lozano, C.J., Haley Jr., P.J., Carniel, S., 2005. A rapid response nowcast/forecast system using multiply nested ocean models and distributed data systems. J. Mar. Syst. 56, 45–66.

Onken, R., Alvarez, A., Fernandez, V., Vizoso, G., Basterretxea, G., Tintore, J., Haley Jr., P. J., Nacini, E., 2008. A forecast experiment in the Balearic Sea. J. Mar. Syst. 71, 79–98.

Pinardi, N., Masetti, E., 2000. Variability of the large scale general circulation of the Mediterranean Sea from observations and modeling: a review. Palaeogeogr. Palaeoclimatol. Palaeoecol. 158, 153–174.

Pinardi, N., Allen, I., Demirov, E., De Mey, P., Korres, G., Lascaratos, A., Le Traon, P.Y., Maillard, C., Manzella, G., Tziavos, C., 2003. The Mediterranean Ocean Forecasting System: first phase of implementation (1998–2001). Ann. Geophys. 21, 3–20.

Pouliquen, E., Kirwan, A.D., Pearson, R.T. (eds.), 1997. Rapid environmental assessment, Lerici, Italy, 10–14 March 1997, SACLANTCEN Conference Proceedings Series CP-44.

Rixen, M., Ferreira-Coelho, E., 2006. Operational prediction of acoustic properties in the ocean using multi-model statistics. Ocean Model. 11 (3–4), 428–440.

Rixen, M., Ferreira-Coelho, E., 2007. Operational surface drift prediction using linear and non-linear hyper-ensemble statistics on atmospheric and ocean models. J. Mar. Syst. 65, 105–121.

Rixen, M., Ferreira-Coelho, E., Signell, R., 2008. Surface drift prediction in the Adriatic Sea using hyper-ensemble statistics on atmospheric, ocean and wave models: uncertainties and probability distribution areas. J. Mar. Syst. 69, 86–98. doi:10.1016/j.jmarsys.2007.02.015.

Rixen, M., Le Gac, J.-C., Hermand, J.-P., Peggion, G., 2009. Super-ensemble forecasts and resulting acoustic sensitivities in shallow waters. J. Mar. Syst. 78, S290–S305 (this issue).

Robinson, A.R., 1999. Forecasting and simulating coastal ocean processes and variabilities with the Harvard Ocean Prediction System. In: Mooers, C.N.K. (Ed.), Coastal Ocean Prediction. AGU Coastal and Estuarine Studies Series. American Geophysical Union, pp. 77–100.

Robinson, A.R., Lermusiaux, P.F.J., 2001. "Data assimilation in models". Encyclopedia of Ocean Sciences. Academic Press Ltd., London, pp. 623–634.

Robinson, A.R., Sellschopp, J., 2002. Rapid assessment of the coastal ocean environment. In: Pinardi, N., Woods, J.D. (Eds.), Ocean forecasting: conceptual basis and applications. Springer, pp. 203–232.

Robinson, A.R., Lermusiaux, P.F.J., 2004. Prediction systems with data assimilation for coupled ocean science and ocean acoustics. In: Tolstoy, A., et al. (Ed.), Keynote manuscript. Proc. of the Sixth International Conference on Theoretical and Computational Acoustics. World Scientific, pp. 325–342.

Robinson, A.R., Arango, H.G., Warn-Varnas, A., Leslie, W.G., Miller, A.J., Haley Jr., P.J., Lozano, C.J., 1996. Real-time regional forecasting. modern approaches to data assimilation in ocean modeling. In: Malanotte-Rizzoli, P. (Ed.), Elsevier Oceanography Series. Elsevier Science, The Netherlands, pp. 377–412.

Robinson, A.R., Abbot, P., Lermusiaux, P.F.J., Dillman, L., 2002. Transfer of uncertainties through physical–acoustical–sonar end-to-end systems: a conceptual basis (.doc). In: Pace, N.G., Jensen, F.B. (Eds.), Acoustic Variability, 2002. SACLANTCEN. Kluwer Academic Press, pp. 603–610.

Schippers, P., 1995. The ALMOST PC model for propagation and reverberation in range dependent environments, Proceedings of UDT Europe.

Wang, D., Lermusiaux, P.F.J., Haley, P.J., Leslie, W.G., Schmidt, H., 2006. Adaptive acoustical-environmental assessment for the focused acoustic field-05 at-sea exercise. Proceedings of IEEE/MTS Oceans'06 Conference, Boston, MA, September 18–21. 6 pp.

Wang, D., Lermusiaux, P.F.J., Haley, P.J., Eickstedt, D., Leslie, W.G., Schmidt, H., 2009. Acoustically focused adaptive sampling and on-board routing for marine rapid environmental assessment. In: Book, J.W., Orlic, M., Rixen, M. (Eds.), Journal of

Marine Systems, Special issue on "MREA and Coastal processes: challenges for monitoring and prediction", vol. 78, pp. S393–S407 (this volume).
Warn-Varnas, A., Sellschopp, J., Haley, P.J., Leslie, W.G., Lozano, C.J., 1999. Strait of Sicily water masses. Dyn. Atm. Oc. 29, 437–469.
Xu, J., Lermusiaux, P.F.J., Haley, P.J. Jr., Leslie, W.G., Logutov, O.G., 2008. Spatial and temporal variations in acoustic propagation during the PLUSNet'07 exercise in Dabob Bay. Proceedings of Meetings on Acoustics (POMA). 155th Meeting, 4, 11. doi:10.1121/1.2988093.
Yilmaz, N.K., Evangelinos, C., Lermusiaux, P.F.J., Patrikalakis, N., 2008. Path planning of AUVs for adaptive sampling using mixed integer linear programming. IEEE Transactions, J. Oceanic Eng. 33 (4), 522–537. doi:10.1109/JOE.2008.2002105.